

**M. V. P. Chowdary<sup>1,2</sup>**

**K. Kalyan Kumar<sup>1,2</sup>**

**Jacob Kurien<sup>2</sup>**

**Stanley Mathew<sup>3</sup>**

**C. Murali Krishna<sup>1</sup>**

*Received 3 May 2006;*

*revised 15 July 2006;*

*accepted 2 August 2006*

*Published online 8 August 2006 in Wiley InterScience (www.interscience.wiley.com). DOI 10.1002/bip.20586*

---

## **Discrimination of Normal, Benign, and Malignant Breast Tissues by Raman Spectroscopy**

# Raman Spectroscopy

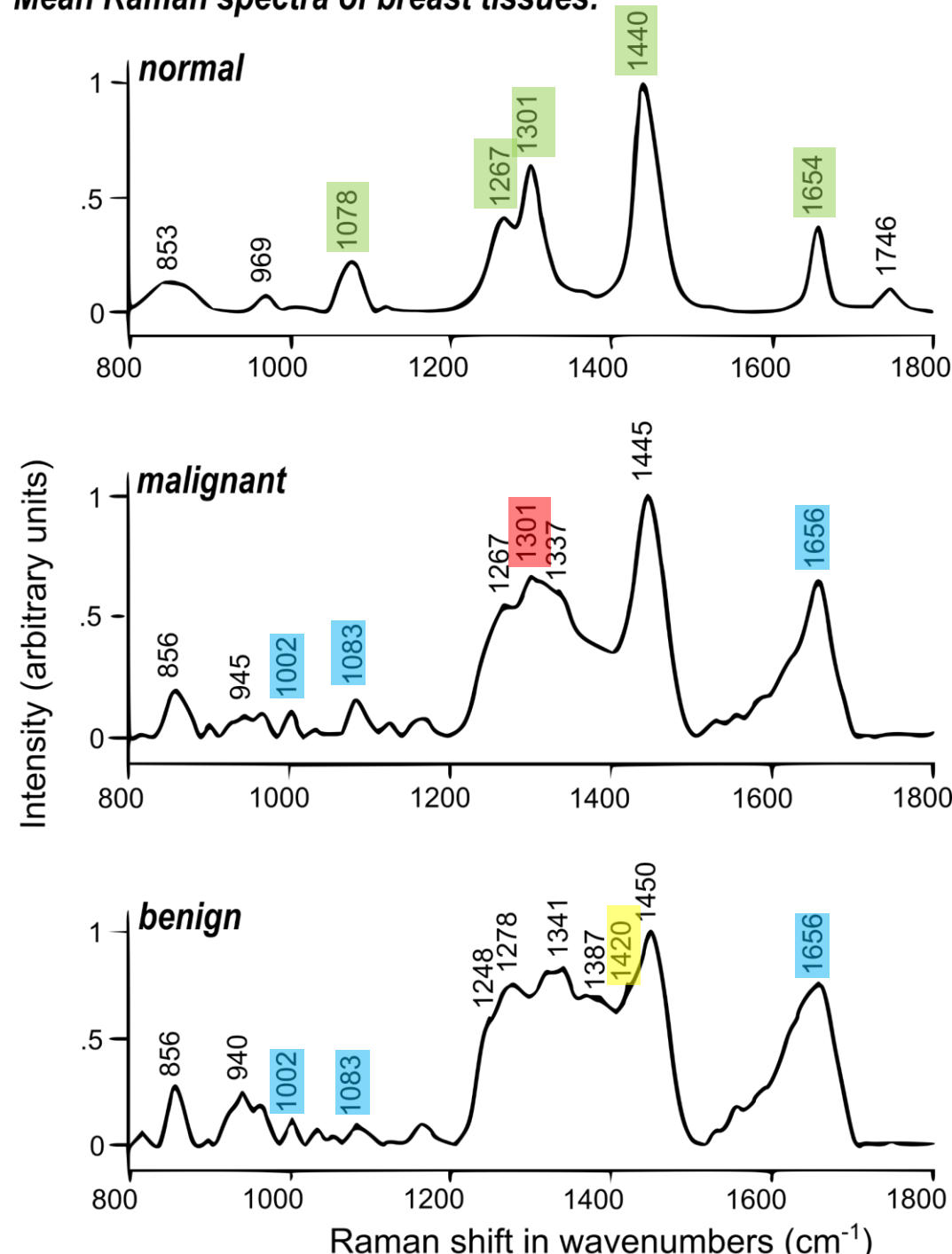
## <paper review>

Antonio Osamu Katagiri Tanaka  
A01212611@itesm.mx

13 Mar 2020



# Mean Raman spectra of breast tissues:



- The spectral profile of normal tissues is indicative of higher levels of lipids (1078, 1267, 1301, 1440, 1654, 1746  $\text{cm}^{-1}$ ). In comparison, the spectral profile of pathological tissues, both benign and malignant, indicates the presence of more proteins (amide I, red shifted DCH2, and amide III, 1002, 1083, 1656  $\text{cm}^{-1}$ ) and fewer lipids.
- Further, among the pathological tissues, malignant tissue contains relatively more lipids (1301  $\text{cm}^{-1}$ ) in comparison to benign tissue.

A total of 258 spectra (105 normal, 101 malignant, 52 benign) from 29 normal, 24 malignant, and 7 benign subjects were studied in the study



M. V. P. Chowdary<sup>1,2</sup>

K. Kalyan Kumar<sup>1,2</sup>

Jacob Kurien<sup>2</sup>

Stanley Mathew<sup>3</sup>

C. Murali Krishna<sup>1</sup>

<sup>1</sup>Center for Laser  
Spectroscopy, Manipal  
Academy of Higher Education,  
Manipal-576 104,  
Karnataka, India

<sup>2</sup>Department of Surgical  
Oncology, Shirdi Sai Baba  
Cancer Hospital and Research  
Center, Manipal Academy of  
Higher Education, Manipal-576  
104, Karnataka, India

<sup>3</sup>Department of General  
Surgery, Kasturba Medical  
College, Manipal Academy of  
Higher Education, Manipal-576  
104, Karnataka, India

Received 3 May 2006;

revised 15 July 2006;

accepted 2 August 2006

Published online 8 August 2006 in Wiley InterScience (www.interscience.wiley.com). DOI 10.1002/bip.20586

## Discrimination of Normal, Benign, and Malignant Breast Tissues by Raman Spectroscopy

**Abstract:** Breast cancers are the leading cancers among females. Diagnosis by fine needle aspiration cytology (FNAC) is the gold standard. The widely practiced screening method, mammography, suffers from high false positive results and repeated exposure to harmful ionizing radiation. As with all other cancers survival rates are shown to heavily depend on stage of the cancers (Stage 0, 95%; Stage IV, 75%). Hence development of more reliable screening and diagnosis methodology is of considerable interest in breast cancer management. Raman spectra of normal, benign, and malignant breast tissue show significant differences. Spectral differences between normal and diseased breast tissues are more pronounced than between the two pathological conditions, malignant and benign tissues. Based on spectral profiles, the presence of lipids (1078, 1267, 1301, 1440, 1654, 1746  $\text{cm}^{-1}$ ) is indicated in normal tissue and proteins (stronger amide I, red shifted  $\Delta\text{CH}_2$ , broad and strong amide III, 1002, 1033, 1530, 1556  $\text{cm}^{-1}$ ) are found in benign and malignant tissues. The major differences between benign and malignant tissue spectra are malignant tissues seem to have an excess of lipids (1082, 1301, 1440  $\text{cm}^{-1}$ ) and presence of excess proteins (amide I, amide III, red shifted  $\Delta\text{CH}_2$ , 1033, 1002  $\text{cm}^{-1}$ ) is indicated in benign spectra. The multivariate statistical tool, principal components analysis (PCA) is employed for developing discrimination methods. A score of factor 1 provided a reasonable classification of all three tissue types. The analysis is further fine-tuned by employing Mahalanobis distance and spectral residuals as discriminating parameters. This approach is tested both retrospectively and prospectively. The limit test, which provides the

Correspondence to: C. Murali Krishna; e-mail: cm.krishna@manipal.edu, krishna.murali@univ-reims.fr

Biopolymers, Vol. 83, 556–569 (2006)

© 2006 Wiley Periodicals, Inc.



most unambiguous discrimination, is also considered and this approach clearly discriminated all three tissue types. These results further support the efficacy of Raman spectroscopic methods in discriminating normal and diseased breast tissues. © 2006 Wiley Periodicals, Inc. *Biopolymers* 83: 556–569, 2006

*This article was originally published online as an accepted preprint. The “Published Online” date corresponds to the preprint version. You can request a copy of the preprint by emailing the Biopolymers editorial office at biopolymers@wiley.com*

**Keywords:** Raman spectroscopy; PCA; breast cancer

## INTRODUCTION

Breast cancer is the most commonly diagnosed malignancy of women (23% of all cancers), ranking overall second when both sexes are considered.<sup>1</sup> The incidence of breast carcinoma is increasing at the rate of 1–2% annually. Prognosis and survival is shown to heavily depend on the stage of diagnosis. Conventional diagnostic methods, clinical examination, and mammography have well-described limitations. These include poor detection of cancerous lesions in younger women or those with radiologically dense breast and a risk of repeated exposure to the harmful ionizing radiations. Mammography may detect 70 to 90% of patients with breast cancer<sup>2</sup> with a false negative rate of up to 31%.<sup>3,4</sup> Fine needle aspiration cytology (FNAC) is the gold standard for confirmation of the diagnosis. Breast biopsy involves surgical excision (removal of entire lesion), core biopsy, and FNAC to ensure proper sampling.<sup>5</sup> Thus the present clinical diagnostic regime, at times, involves multiple biopsies with time delayed results. Therefore, there exists considerable interest in developing fast, less invasive, objective methods for diagnosis and screening of breast cancers.

Optical spectroscopic techniques<sup>6–17</sup> are fast emerging as promising alternatives in biology and medicine, including cancer diagnosis. Breast cancer diagnosis by spectroscopic methods such as fluorescence,<sup>6–8</sup> reflectance,<sup>9</sup> and Raman<sup>10–17</sup> are reported in the literature. Many of the Raman spectroscopy studies that appeared in the literature have employed a microspectroscopic approach.<sup>10–15</sup> These studies indicated very good discrimination of normal and pathological conditions. In most of these investigations, normal spectra are dominated by lipids whereas an abundance of proteins is seen in pathological tissues. Microspectroscopy provides better understanding of biochemical composition as spectra can be recorded from the selected regions.<sup>18</sup> On the other hand, conventional Raman spectroscopy has the advantage of simulating in situ/in vivo conditions using ex vivo samples. In this approach spectra that are representative as signals are collected from a

larger region. Thus, the results can be extrapolated to in vivo/in situ conditions.

Raman spectroscopy offers certain distinct advantages over other optical diagnostic techniques such as fluorescence and FTIR. The advantages include high spatial resolution (down to 1  $\mu\text{m}$ ) in the microspectroscopic model, use of less harmful NIR radiation, less or no sample preparation, and no influence of water bands, which facilitates in vivo/in situ measurements. Despite these advantages not many Raman spectroscopic studies pertaining to diagnosis of cancer are reported in the literature.

As can be seen from the literature, mentioned above, few groups have investigated the feasibility of diagnosing breast cancers by Raman spectroscopy.<sup>10–17</sup> However, for clinical application, it is necessary that a methodology is verified and validated by different groups to establish the approach before employing it for routine use. In view of these considerations, Raman spectroscopy of normal, benign, and malignant breast tissues of an Indian population are carried out. To the best of our knowledge, this is the first report on Raman spectroscopy-based diagnosis of breast cancers among an Indian population. In the present study, Raman spectra of normal, benign, and malignant tissues are recorded. PCA is used as the multivariate statistical tool for the data analysis. Scores of factors, Mahalanobis distance, and spectral residuals are used as discriminating parameters. Further a multiparametric “limit test” approach is also considered to develop more objective and unambiguous discrimination. The results obtained are presented and discussed in the paper.

## MATERIALS AND METHODS

Breast tissue samples, routine surgical resections, or biopsies were obtained in saline from the Department of Surgical Oncology, Shirdi Sai Baba Cancer Hospital, and Research Center, MAHE, Manipal, India and Department of General Surgery, Kasturba Hospital, MAHE, Manipal, India. Tissue from uninvolved areas from the same subjects was used as control/normal. A mirror image of each sample was sent for histopathological certification. Spectra were

**Table I** Details of Samples Used in the Study

Standard Samples		
Spectrum Number	Nature	Histopathology
1–105	Normal	Normal
106–206	Malignant	Malignant
207–258	Fibroadenoma	Fibroadenoma

recorded at six or more different sites on each tissue sample. Only good spectra from clear normal, malignant, and benign tissues were employed for analysis. A total of 258 sites/spectra (105 normal, 101 malignant, 52 benign) from 29 normal, 24 malignant, and 7 benign subjects were recruited in the study. Details of the samples used in the study are shown in the Table I.

### Laser Raman Spectroscopy

Raman spectra were recorded using the set up assembled by us.<sup>19–21</sup> This setup consisted of a diode laser (785 nm, SDL diode laser 8530, 150 mW) for excitation. Raman signals were detected by combination of spectrometer (Spex Triax 320, 600 g/mm, blazed at 900 nm) and Spectrum one liquid nitrogen cooled CCD (Jobin Yvon-Spex, Instruments S.A., Inc.). A holographic filter (HLBF-785.0, Kaiser Optics, Ann Arbor, MI, USA) was used to reject unwanted lines from the excitation source. Rayleigh scattering was removed by a notch filter (HSPF-5812, Kaiser Optics, Ann Arbor, MI, USA). Other experimental conditions were integration time – 30 s and number of accumulations – 20. These settings were kept constant for all the measurements. The recorded spectra were calibrated with a cubic fit to known frequencies of Tylenol (4-acetamidophenol).

### Data Analysis

Baseline correction, smoothing, calibration, and normalization with respect to  $\Delta\text{CH}_2$  band were carried out using algorithms of Grams 32 (Galactic Industries Corporation, Salem, NH, USA). PCA was carried out using Grams PLS Plus (Galactic Industries Corporation). PCA was carried out under different conditions: different number of factors, entire range (800–1800  $\text{cm}^{-1}$ ), several selected regions, derivative spectra to explore the best discrimination. In our analysis, the 1400–1750  $\text{cm}^{-1}$  spectral region with nine factors provided the best discrimination. Further analysis was carried out under these conditions.

## RESULTS AND DISCUSSION

The mean Raman spectra of normal, malignant, and benign tissues showed very significant differences (Figure 1). Differences between spectra profiles of normal and pathological conditions were more pronounced compared with those between the two patho-

logical conditions, benign and malignant. The spectral features of normal tissue, bands at around 1078, 1267, 1301, 1440, 1654, and 1746  $\text{cm}^{-1}$ , were assigned to vibrational modes of lipids (Figure 1a). The spectral profiles of benign and malignant tissues, strong amide I, broad amide III, and peaks at 1002, 1083, 1530, and 1556  $\text{cm}^{-1}$  were attributed to vibrational modes of proteins (Figure 1b and 1c). The major differences between benign spectra with respect to malignant spectra are: red shifted and broad  $\Delta\text{CH}_2$  peak, relatively strong amide I, and stronger and broader amide III (Figure 1c). All of the observed spectral features may provide vital clues in understanding the differences in the biochemical composition of tissues.

To bring out the differences in spectral profiles more clearly, difference spectra were computed by subtracting mean normal spectrum from mean malignant and benign spectra, respectively (Figure 2a and b). All of the negative peaks, 1066, 1301, 1437, and 1744  $\text{cm}^{-1}$ , were due to normal spectrum and these spectral features can be assigned to lipids. The positive peaks in Figure 2a and b were due to malignant and benign spectra, respectively. Most of the positive bands seen around 857, 940, 1002, 1033, 1169, 1244, 1281, 1341, 1381, 1417, 1465, 1530, 1556, 1587, 1637, and 1666  $\text{cm}^{-1}$  can be assigned to different

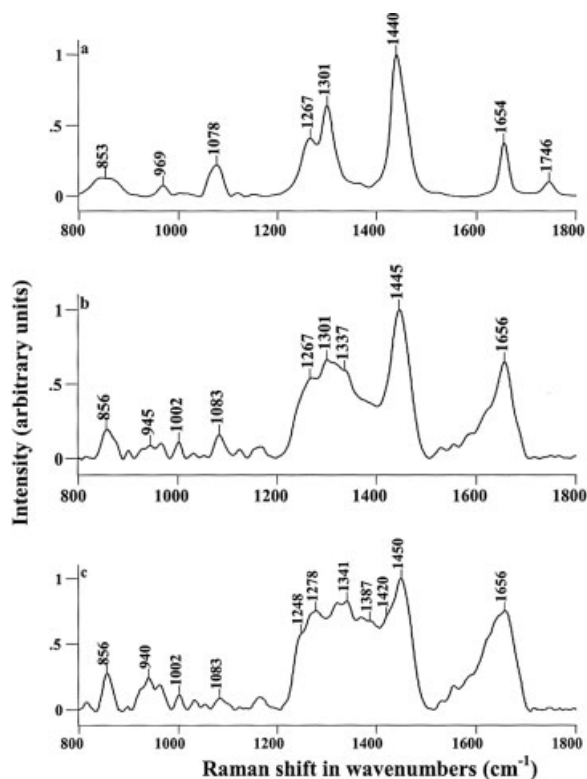


**FIGURE 1** Mean Raman spectra of breast tissues: (a) normal; (b) malignant; (c) benign.

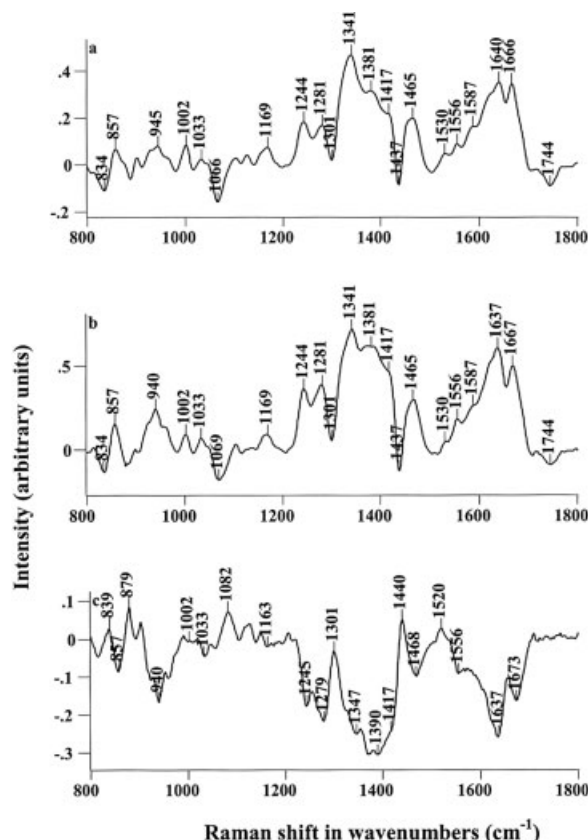


**FIGURE 2** Difference spectra of normal, malignant, and benign breast tissue spectra: (a) malignant – normal; (b) benign – normal; (c) malignant – benign.

vibrational modes of backbone and amino acid residues of proteins. As mentioned earlier, the differences between spectral profiles of benign and malignant are less pronounced compared with those between normal and pathological tissues. This is clearly evident from the difference spectra (Figure 2). The bands in difference spectrum Figure 2c, which was computed by subtracting the mean benign spectrum from the mean malignant spectrum, were relatively weak compared with the other two difference spectra (Figure 2a and b). In this spectrum, Figure 2c, all of the negative peaks were due to the benign spectrum. Many of these features, bands around 857, 940, 1002, 1033, 1163, 1245, 1279, 1347, 1390, 1468, 1556, 1634, and 1673  $\text{cm}^{-1}$  can be assigned to proteins, which indicates the presence of excess proteins in the benign spectrum. The positive peaks around 839, 879, 1082, 1301, and 1440  $\text{cm}^{-1}$ , which were contributed by the malignant spectrum, could be due to lipids. All of the vibrational modes observed in Raman spectra of normal, malignant, and benign tissues were assigned based on available literature data.<sup>22,23</sup> These spectral features, dominance of lipids in the normal spectrum and high protein content

in malignant tissues, corroborate findings of earlier studies.<sup>10–17</sup> To verify the variability within the same tissue, i.e., normal, benign, and malignant, spectra from the same tissue corresponding to respective tissue type were overlapped as shown in Figure 3. As can be seen from the figure, the variability within a particular tissue type is very subtle, as expected, it is limited to minor intensity variations without any significant change in the profile of the spectra.

One of the major advantages of spectroscopic diagnosis is high objectivity. This is facilitated by the fact that the spectra are amenable to multivariate statistical tools such as PCA, artificial neural network (ANN), and hierarchical cluster analysis (HCA). In the present studies, two approaches were considered to obtain discrimination among the three classes of samples, namely, normal, benign, and malignant. In the first approach, spectra of all three classes of samples were pooled and analyzed by PCA. Scores of factors were explored for discrimination. In PCA, large spectral data are decomposed into small number of independent variations known as Factors or Principal Components and contributions of these factors are known as Scores. Scores of factors is one of the widely used parameters for classification. As mentioned earlier, the selected region of 1400–1750  $\text{cm}^{-1}$  gave the best discrimination. Plots of % variation versus factors and Eigen val-

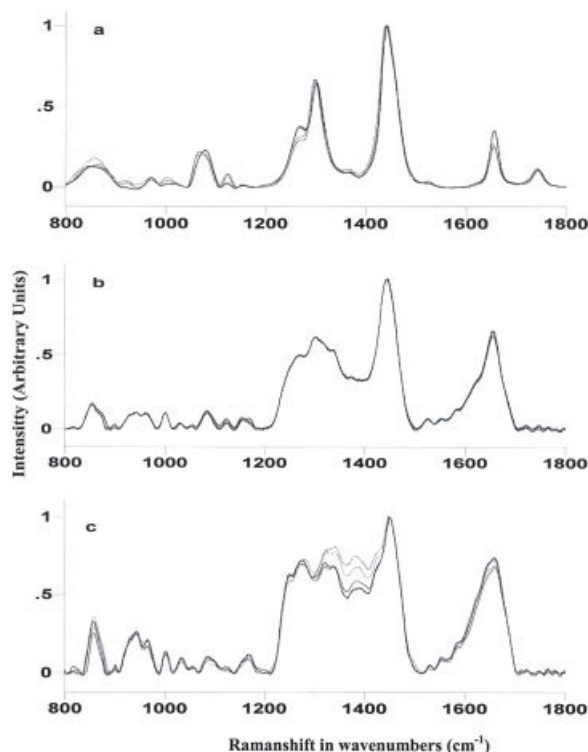


**FIGURE 3** Typical Raman spectral variations within a tissue in breast tissues: (a) normal; (b) malignant; (c) benign.

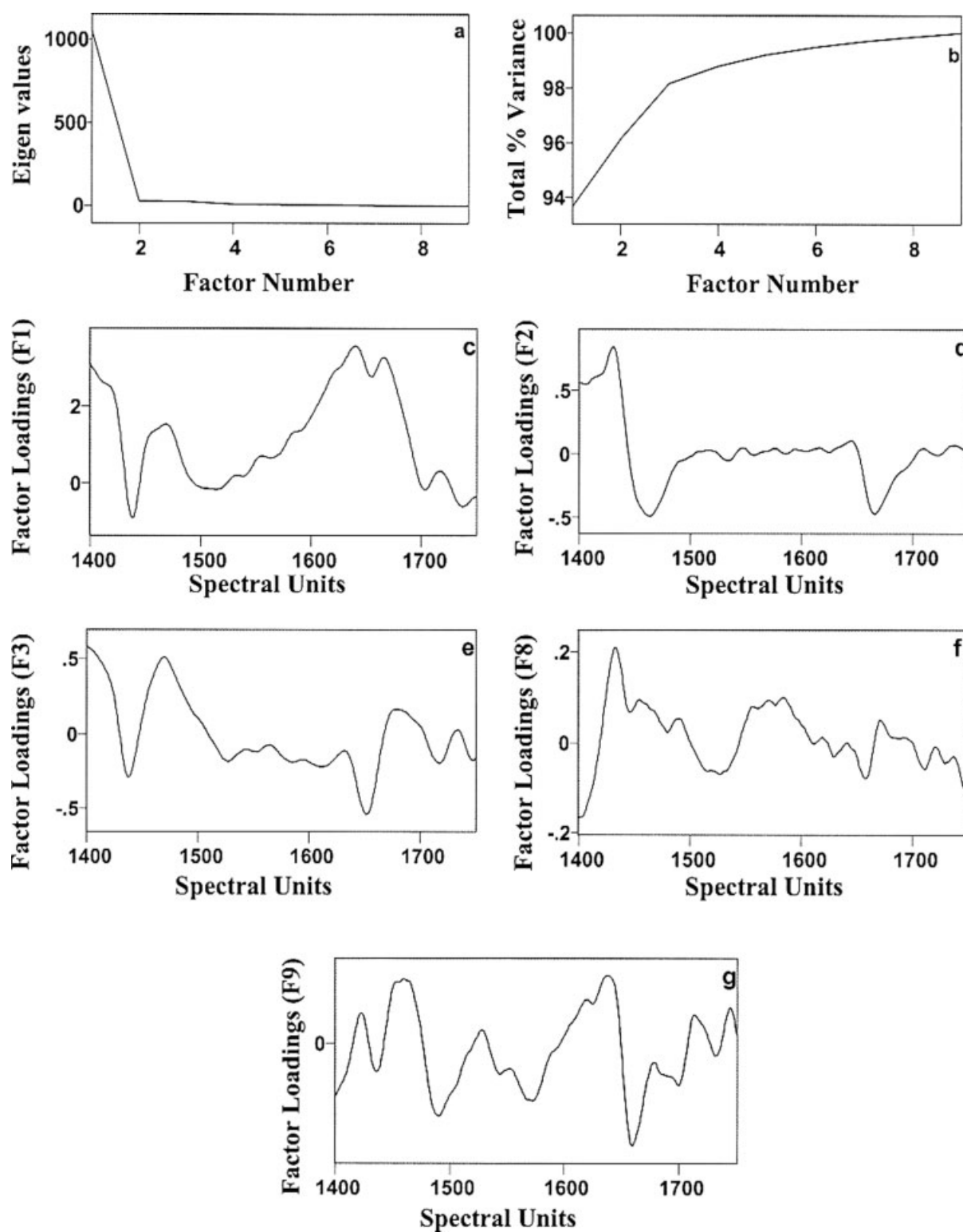


**FIGURE 4** PCA of normal, malignant, and benign Raman spectra of breast tissue: (a) Eigen value plot; (b) total % variance; (c) loadings of factor 1; (d) loadings of factor 2; (e) loadings of factor 3; (f) loadings of factor 8; (g) loadings of factor 9.

**Table II** PCA of Raman Spectra of Normal, Malignant, and Benign Breast Tissues: Eigen values, Total % Variance

Factor Number	Eigen Value	Total % Variance
1	1047.349	93.67731
2	27.7394	96.15838
3	22.31309	98.15412
4	7.245638	98.80218
5	4.583775	99.21217
6	3.097776	99.48924
7	2.279846	99.69315
8	1.869763	99.86039
9	1.560891	100

ues versus factors are shown in Figure 5. The first three factors accounted for 98% variation in the spectra (Table II). Profiles of factors, “factor loads,” of the first three factors and the last two factors are shown in Figure 4. In our analysis, scores of factor 1 provided a reasonable classification among three groups (Figure 4). As can be seen from the figure, the contribution of factor 1 is negative for normal spectra and largely positive for benign and malignant spectra. Cluster of malignant spectra occupy between clusters corresponding to normal and benign tissues. The mean and standard deviations of score of factor 1 for normal, malignant, and benign spectra are  $-0.068 \pm 0.006$ ,  $0.028 \pm 0.023$ , and  $0.083 \pm 0.007$ , respectively. Thus a reasonable classification of three clusters can be seen up to mean  $\pm 1$  standard deviation, which indicates 75% sensitivity/specificity.

The classification based on scores of factor though a widely used approach could be subjective as discriminating components are selected. Generally algorithms of discriminant analysis are used to identify the most discriminating factors or principal components.<sup>18</sup> However, this may not provide a very good classification under all circumstances.<sup>19–21</sup> In view of this we have considered another approach. In this second approach, standard sets of each class, normal, malignant, and benign, using pathologically certified samples were developed. Spectral residuals (sum of the squares of the difference between observed and simulated spectra) and Mahalanobis distance (measured in terms standard deviation from mean of the training set) were computed for the spectra against the standard sets in both retrospective as well as prospective modality. And these parameters have been explored to achieve better discrimination of tissue type. This approach has been successfully employed by us for discrimination of oral and cervical tissues.<sup>19–21</sup> The mathematical basis of the Mahalanobis distance calculation is well known<sup>24–26</sup> and widely used for spectral discrimination. It is very sensitive to intervariable changes in the calibration data and it is measured in terms of standard deviations from the mean of the training samples. In addition to providing spectral discrimination, it also gives a statistical measure of how well the unknown sample spectrum matches or does not match. Thus it is a statistical measure of proximity of two spectra. In the present analysis, Mahalanobis distance is coupled with PCA, which is a very effective data reduction technique for

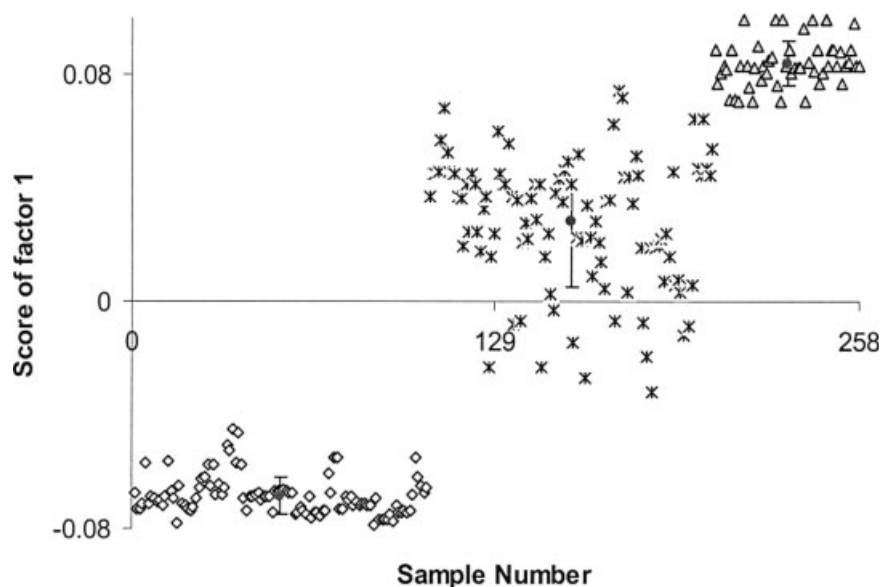


**FIGURE 5** PCA of Raman spectra of normal, malignant, and benign breast tissues.  $\diamond$  Normal; \* Malignant;  $\blacktriangle$  Benign.



spectroscopic data and thus allows full spectral coverage for all samples. In our analysis, Mahalanobis distance is computed using the expression

$$D^2 = (S_{\text{test}}) M^{-1} (S_{\text{test}})'$$

Where  $S_{\text{test}}$  is the vector of the scores and sum of squared spectral residuals for a given test sample, and  $M$  is an  $f$  by  $f$  Mahalanobis matrix given by  $M = \frac{S' S}{(n-1)}$ , where  $S$  contains the corresponding parameters for the calibration set ( $n$  standards).

The advantages of using  $D^2$  as a discriminating parameter are described elsewhere.<sup>23–25</sup> Mahalanobis distance and spectral residuals are computed by matching spectra against normal, malignant, and be-

nign standard sets. Randomly picked spectra based on scores of factor 1 and pathological certifications are employed to develop standard calibration sets for normal (36 spectra), malignant (35 spectra), and benign (21 spectra) conditions. The standard sets were verified retrospectively where spectra from the standard sets are matched to compute Mahalanobis distance and spectral residuals. It is expected that if spectra and standard sets are of same class, values for Mahalanobis distance and spectral residuals are low and vice versa. As an example, retrospective analysis against normal standard is shown in Figure 6. As can be seen from the figure, very good classification of tissue type is achieved. Mahalanobis distance for all normal spec-

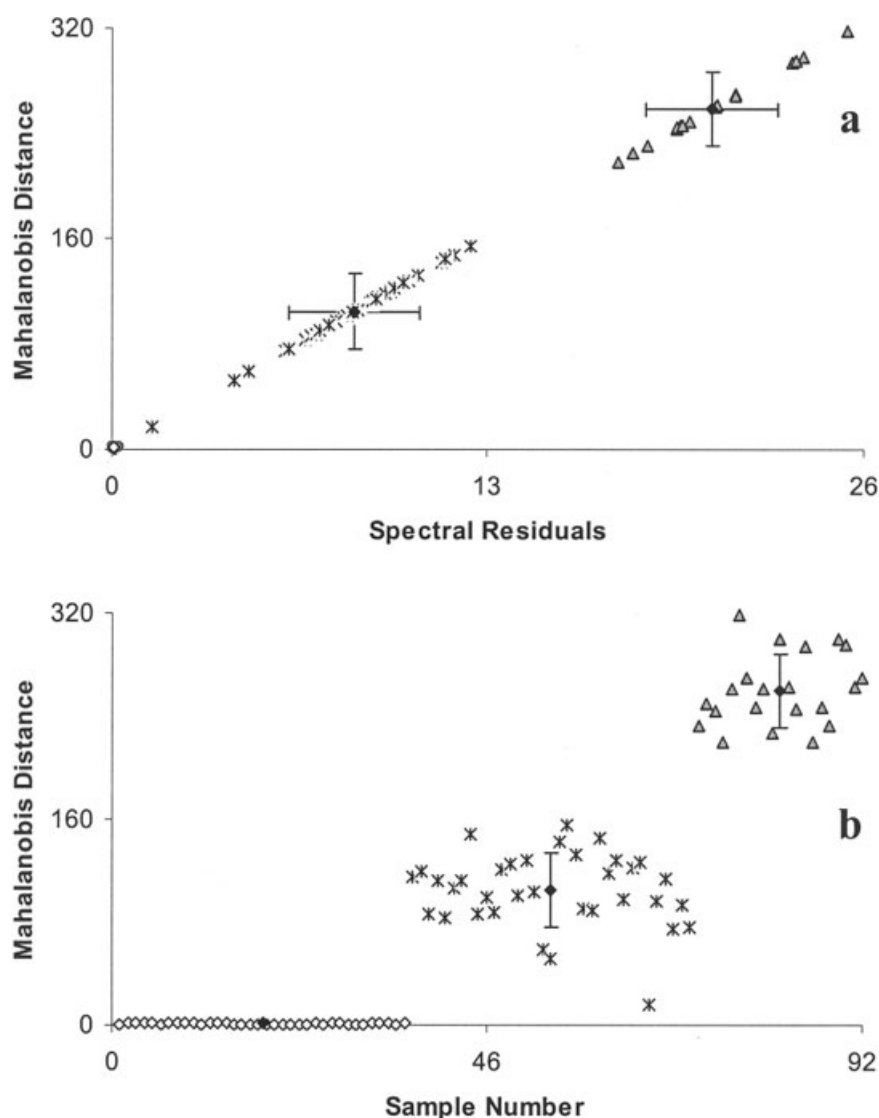


**FIGURE 6** PCA of Raman spectra of breast tissue—retrospective study against normal standard set: (a) plot of spectral residual versus Mahalanobis distance; (b) plot of sample number versus Mahalanobis distance. ◇ Normal; \* Malignant; ▲ Benign.

tra are around  $0.881 \pm 0.44$ , and values for malignant and benign spectra are around  $104.42 \pm 28.64$  and  $259.85 \pm 28.43$ , respectively. Spectral residual values for normal spectra are around  $0.09 \pm 0.05$  and for malignant and benign spectra are around  $8.40 \pm 2.27$  and  $20.76 \pm 2.26$ , respectively. The approach was evaluated prospectively, matching all normal, benign, and malignant spectra that were not included in the standard sets, against standard sets. Typical results obtained in prospective analysis against malignant standard sets are shown in Figure 7. The clear clustering, barring minor overlap among the clusters, which could not be assigned pathological status, obtained in the analysis validates standard sets. Mean Mahalanobis distance for all malignant spectra were around  $1.19 \pm 0.64$ , and values for benign and normal spectra around  $5.53$

$+ 1.24$  and  $10.52 \pm 1.75$ , respectively. Spectral residual values for malignant, benign and normal spectra were around  $0.65 \pm 0.40$ ,  $2.60 \pm 0.56$  and  $5.23 \pm 1.24$ , respectively.

The above approach was further extended to compute match/mismatch tables or a "Limit test," which is considered to obtain unambiguous discrimination of tissue types. This methodology is successfully applied to discriminate normal, inflammatory, premalignant, and malignant oral tissues and normal and malignant conditions of the cervix.<sup>19–21</sup> In this methodology, spectra are matched against standard sets with inclusions/exclusions set for three discrimination parameters: scores of factors, Mahalanobis distance, and spectral residuals. If the values of the given spectrum fall within set limits, spectra show YES or PASS,

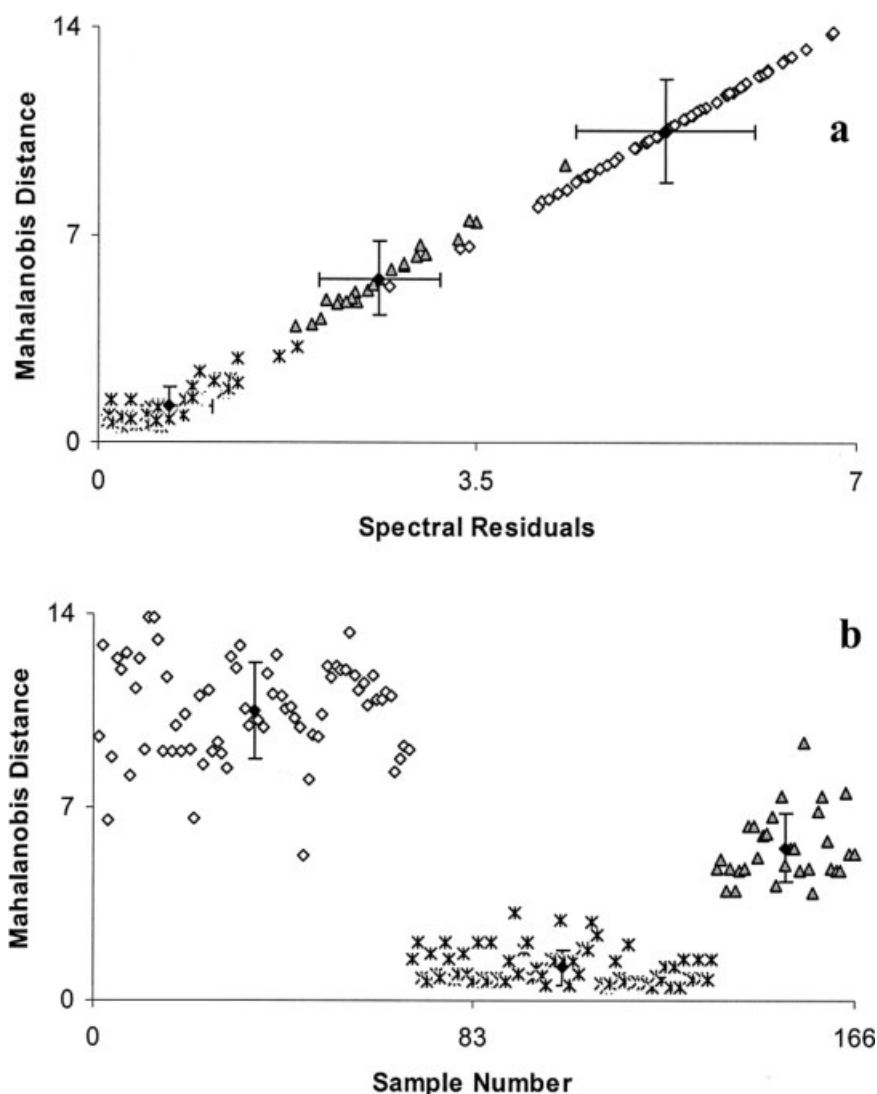


**FIGURE 7** PCA of Raman spectra of breast tissues—prospective study against malignant standard set: (a) plot of spectral residual versus Mahalanobis distance; (b) plot of sample number versus Mahalanobis distance.  $\diamond$  Normal;  $*$  Malignant;  $\blacktriangle$  Benign.

**Table III** Multiparametric Match/Mismatch Table Compared Against Benign Standard Set

Sample Number	Match	Mahalanobis Distance	Limit Tests	Spectral Residual
1	No	154.52246	Fail (PFF#)	24.151834
2	No	166.45626	Fail (PFF#)	26.039245
3	No	165.6464	Fail (PFF#)	25.893308
4	No	162.32982	Fail (PFF#)	25.382414
5	No	134.07467	Fail (PFF#)	20.986553
6	No	162.64674	Fail (PFF#)	25.428597
7	No	157.47355	Fail (PFF#)	24.635371
8	No	158.44057	Fail (PFF#)	24.779253
9	No	159.83266	Fail (PFF#)	24.994801
10	No	159.37699	Fail (PFF#)	24.921713
11	No	162.6142	Fail (PFF#)	25.426248
12	No	157.60521	Fail (PFF#)	24.652342
13	No	131.16563	Fail (PFF#)	20.562932
14	No	151.691	Fail (PFF#)	23.748195
15	No	156.93794	Fail (PFF#)	24.567031
16	No	176.3405	Fail (PFF#)	27.573818
17	No	148.19333	Fail (PFF#)	23.214416
18	No	161.72258	Fail (PFF#)	25.300577
19	No	164.22728	Fail (PFF#)	25.689614
20	No	165.62013	Fail (PFF#)	25.903564
21	No	167.03384	Fail (PFF#)	26.124753
22	No	164.3466	Fail (PFF#)	25.70915
23	No	157.53945	Fail (PFF#)	24.651057
24	No	149.76166	Fail (PFF#)	23.433988
25	No	144.80625	Fail (PFF#)	22.665443
26	No	143.732	Fail (PFF#)	22.498237
27	No	133.58811	Fail (PFF#)	20.925826
28	No	149.64087	Fail (PFF#)	23.404721
29	No	133.97002	Fail (PFF#)	20.984014
30	No	154.35693	Fail (PFF#)	24.150431
31	No	147.04683	Fail (PFF#)	23.013104
32	No	154.66193	Fail (PFF#)	24.196715
33	No	149.92767	Fail (PFF#)	23.461226
34	No	122.29226	Fail (PFF#)	19.194846
35	No	125.49122	Fail (PFF#)	19.682771
36	No	111.86007	Fail (PFF#)	17.568149
37	No	135.13666	Fail (PFF#)	21.177365
38	No	115.80469	Fail (PFF#)	18.170427
39	No	136.49853	Fail (PFF#)	21.387595
40	No	157.53945	Fail (PFF#)	24.651057
41	No	166.14668	Fail (PFF#)	25.986709
42	No	158.07804	Fail (PFF#)	24.706919
43	No	157.88281	Fail (PFF#)	24.675314
44	No	156.44336	Fail (PFF#)	24.455824
45	No	154.94271	Fail (PFF#)	24.222595
46	No	158.96237	Fail (PFF#)	24.845705
47	No	156.19518	Fail (PFF#)	24.415974
48	No	157.04216	Fail (PFF#)	24.550775
49	No	156.82689	Fail (PFF#)	24.515457
50	No	168.44621	Fail (PFF#)	26.315474
51	No	152.94638	Fail (PFF#)	23.907725
52	No	152.60167	Fail (PFF#)	23.851668
53	No	153.20453	Fail (PFF#)	23.947045
54	No	151.95531	Fail (PFF#)	23.753628

(Continued)

**Table III** (Continued from the previous page.)

Sample Number	Match	Mahalanobis Distance	Limit Tests	Spectral Residual
55	No	153.19782	Fail (PFF#)	23.94453
56	No	153.76303	Fail (PFF#)	24.033135
57	No	154.52246	Fail (PFF#)	24.151834
58	No	169.30983	Fail (PFF#)	26.457941
59	No	168.55814	Fail (PFF#)	26.350382
60	No	163.98942	Fail (PFF#)	25.638539
61	No	166.07914	Fail (PFF#)	25.984536
62	No	168.5125	Fail (PFF#)	26.341428
63	No	155.9306	Fail (PFF#)	24.393914
64	No	171.39882	Fail (PFF#)	26.796937
65	No	167.83373	Fail (PFF#)	26.246916
66	No	168.16938	Fail (PFF#)	26.298465
67	No	172.01048	Fail (PFF#)	26.872543
68	No	166.62991	Fail (PFF#)	26.060579
69	No	166.28094	Fail (PFF#)	26.011062
70	No	139.91296	Fail (PFF#)	21.921439
71	No	154.52246	Fail (PFF#)	24.151834
72	No	129.80808	Fail (PFF#)	20.356054
73	No	128.06179	Fail (PFF#)	20.099773
74	No	166.45626	Fail (PFF#)	26.039245
75	No	165.6464	Fail (PFF#)	25.893308
76	No	156.15936	Fail (PFF#)	24.432674
77	No	158.69514	Fail (PFF#)	24.823467
78	No	155.20604	Fail (PFF#)	24.28653
79	No	162.66834	Fail (PFF#)	25.432695
80	No	160.21848	Fail (PFF#)	25.053339
81	No	162.9888	Fail (PFF#)	25.483686
82	No	161.12346	Fail (PFF#)	25.183213
83	No	161.04602	Fail (PFF#)	25.170668
84	No	162.56282	Fail (PFF#)	25.404399
85	No	162.56282	Fail (PFF#)	25.404399
86	No	178.19598	Fail (PFF#)	27.830032
87	No	157.94923	Fail (PFF#)	24.693513
88	No	173.60286	Fail (PFF#)	27.127591
89	No	173.66463	Fail (PFF#)	27.138237
90	No	173.3279	Fail (PFF#)	27.085481
91	No	173.15514	Fail (PFF#)	27.057981
92	No	169.39683	Fail (PFF#)	26.478632
93	No	174.12861	Fail (PFF#)	27.209825
94	No	165.04634	Fail (PFF#)	25.787529
95	No	168.10887	Fail (PFF#)	26.268448
96	No	168.20897	Fail (PFF#)	26.286019
97	No	166.96542	Fail (PFF#)	26.091291
98	No	167.70928	Fail (PFF#)	26.207637
99	No	167.06289	Fail (PFF#)	26.107231
100	No	155.3238	Fail (PFF#)	24.285134
101	No	128.60533	Fail (PFF#)	20.147898
102	No	142.68863	Fail (PFF#)	22.318912
103	No	148.00253	Fail (PFF#)	23.152701
104	No	153.89957	Fail (PFF#)	24.071532
105	No	149.80185	Fail (PFF#)	23.438586
106	No	16.244087	Fail (PFF#)	2.7172556
107	No	11.58526	Fail (PFF#)	2.0316373
108	No	14.110687	Fail (PFF#)	2.4257418

(Continued)

**Table III** (Continued from the previous page.)

Sample Number	Match	Mahalanobis Distance	Limit Tests	Spectral Residual
109	No	10.228449	Fail (PFF#)	1.7486183
110	No	7.8725281	Fail (P?F#)	1.4200823
111	No	6.9843291	Fail (P?F#)	1.2732269
112	No	11.302798	Fail (PFF#)	1.968387
113	No	10.228449	Fail (PFF#)	1.7486183
114	No	14.110687	Fail (PFF#)	2.4257418
115	No	11.58526	Fail (PFF#)	2.0316373
116	No	16.244087	Fail (PFF#)	2.7172556
117	No	15.681282	Fail (PFF#)	2.6517327
118	No	28.406374	Fail (FFF#)	4.6707034
119	No	12.422363	Fail (PFF#)	2.1603494
120	No	24.794465	Fail (PFF#)	4.0635876
121	No	11.385221	Fail (PFF#)	2.0023184
122	No	12.422363	Fail (PFF#)	2.1603494
123	No	24.794465	Fail (PFF#)	4.0635876
124	No	30.49831	Fail (PFF#)	4.876836
125	No	18.086489	Fail (PFF#)	3.0130556
126	No	16.471775	Fail (PFF#)	2.7447988
127	No	78.166704	Fail (PFF#)	12.306064
128	No	32.993165	Fail (PFF#)	5.2987373
129	No	24.840821	Fail (PFF#)	4.0333362
130	No	6.1116584	Fail (P?F#)	1.1238708
131	No	11.773123	Fail (PFF#)	2.0228927
132	No	13.904603	Fail (PFF#)	2.3101694
133	No	13.904603	Fail (PFF#)	2.3101694
134	No	5.7014316	Fail (P?F#)	1.0943288
135	No	24.831926	Fail (PFF#)	3.9955121
136	No	62.714877	Fail (PFF#)	9.8949026
137	No	17.185709	Fail (PFF#)	2.836669
138	No	56.838813	Fail (PFF#)	8.9967588
139	No	29.018779	Fail (PFF#)	4.6566396
140	No	22.232862	Fail (PFF#)	3.6031636
141	No	26.440053	Fail (PFF#)	4.2671934
142	No	14.782007	Fail (PFF#)	2.5178466
143	No	13.243161	Fail (PFF#)	2.2740299
144	No	20.545113	Fail (PFF#)	3.3621383
145	No	12.250009	Fail (PFF#)	2.0864864
146	No	78.166704	Fail (PFF#)	12.306064
147	No	32.993165	Fail (PFF#)	5.2987373
148	No	24.840821	Fail (PFF#)	4.0333362
149	No	45.012375	Fail (PFF#)	7.173343
150	No	51.733377	Fail (PFF#)	8.2105943
151	No	15.969781	Fail (PFF#)	2.5826447
152	No	13.280632	Fail (PFF#)	2.1621049
153	No	19.125931	Fail (PFF#)	3.0794604
154	No	11.054709	Fail (PFF#)	1.8187381
155	No	8.3843428	Fail (P?F#)	1.47462
156	No	11.802658	Fail (PFF#)	2.0178502
157	No	65.01548	Fail (PFF#)	10.267177
158	No	25.134037	Fail (PFF#)	4.0931434
159	No	5.8629188	Fail (P?F#)	1.1354316
160	No	26.016332	Fail (PFF#)	4.2442661
161	No	83.282837	Fail (PFF#)	13.105609
162	No	20.958097	Fail (PFF#)	3.3950776

(Continued)

**Table III** (Continued from the previous page.)

Sample Number	Match	Mahalanobis Distance	Limit Tests	Spectral Residual
163	No	30.111839	Fail (PFF#)	4.8673111
164	No	45.195132	Fail (PFF#)	7.2167438
165	No	24.757509	Fail (PFF#)	4.0127864
166	No	30.412939	Fail (PFF#)	4.8772424
167	No	37.083359	Fail (PFF#)	5.9257475
168	No	46.100841	Fail (PFF#)	7.3430807
169	No	17.349995	Fail (PFF#)	2.8247216
170	No	17.185709	Fail (PFF#)	2.836669
171	No	17.349995	Fail (PFF#)	2.8247216
172	No	56.838813	Fail (PFF#)	8.9967588
173	No	17.349995	Fail (PFF#)	2.8247216
174	No	17.349995	Fail (PFF#)	2.8247216
175	No	11.90357	Fail (PFF#)	2.0174714
176	No	44.056272	Fail (PFF#)	7.0136503
177	No	11.90357	Fail (PFF#)	2.0174714
178	No	16.609869	Fail (PFF#)	2.7551161
179	No	8.5902449	Fail (P?F#)	1.5159437
180	No	11.824622	Fail (PFF#)	1.996328
181	No	31.888074	Fail (PFF#)	5.1364167
182	No	58.025759	Fail (PFF#)	9.1835259
183	No	72.881859	Fail (PFF#)	11.491003
184	No	31.888074	Fail (PFF#)	5.1364167
185	No	89.840098	Fail (PFF#)	14.146692
186	No	28.38357	Fail (PFF#)	4.5966694
187	No	28.034792	Fail (PFF#)	4.5960093
188	No	29.390382	Fail (PFF#)	4.7889831
189	No	41.017168	Fail (PFF#)	6.5747806
190	No	23.861237	Fail (PFF#)	3.9285166
191	No	31.046557	Fail (PFF#)	5.0192138
192	No	9.7566777	Fail (PFF#)	1.7094075
193	No	42.29662	Fail (PFF#)	6.7052732
194	No	40.909812	Fail (PFF#)	6.5159057
195	No	45.355118	Fail (PFF#)	7.2081141
196	No	62.20789	Fail (PFF#)	9.8502354
197	No	42.29662	Fail (PFF#)	6.7052732
198	No	60.30373	Fail (PFF#)	9.5272639
199	No	42.29662	Fail (PFF#)	6.7052732
200	No	6.9953473	Fail (P?F#)	1.2255174
201	No	10.188441	Fail (PFF#)	1.7553443
202	No	11.574023	Fail (PFF#)	1.9788702
203	No	6.9953473	Fail (P?F#)	1.2255174
204	No	10.188441	Fail (PFF#)	1.7553443
205	No	11.574023	Fail (PFF#)	1.9788702
206	No	6.9953473	Fail (P?F#)	1.2255174
207	Possible	1.2339715	Pass (PP?#)	0.1075388
208	Yes	0.3428911	Pass (PPP#)	0.1512337
209	Yes	0.9878245	Pass (PPP#)	0.04488258
210	Yes	0.5677136	Pass (PPP#)	0.1707019
211	Yes	0.4586411	Pass (PPP#)	0.1704782
212	Yes	0.5472146	Pass (PPP#)	0.2208394
213	Possible	1.2339715	Pass (PP?#)	0.1075388
214	Yes	0.5472146	Pass (PPP#)	0.2208394
215	Yes	0.7996501	Pass (PPP#)	0.2643451
216	Yes	0.8596138	Pass (PPP#)	0.08203353

(Continued)

**Table III** (Continued from the previous page.)

Sample Number	Match	Mahalanobis Distance	Limit Tests	Spectral Residual
217	Possible	1.1667353	Pass (PP?#)	0.2849572
218	Possible	1.2261093	Pass (PP?#)	0.07781574
219	Possible	2.8754408	Pass (PP?#)	0.5887623
220	Yes	0.7996501	Pass (PPP#)	0.2643451
221	Possible	1.0471809	Pass (PP?#)	0.1386804
222	Yes	0.8659271	Pass (PPP#)	0.07630237
223	Yes	0.4925431	Pass (PPP#)	0.12101
224	Yes	0.8596138	Pass (PPP#)	0.08203353
225	Yes	0.8691097	Pass (PPP#)	0.0751665
226	Possible	1.2889638	Pass (PP?#)	0.02532688
227	Possible	1.4717093	Pass (PP?#)	0.4113595
228	Possible	1.1667353	Pass (PP?#)	0.2849572
229	Yes	0.2196176	Pass (PPP#)	0.1913339
230	Yes	0.7425372	Pass (PPP#)	0.3260033
231	Possible	1.1876442	Pass (PP?#)	0.3833324
232	Yes	0.8892672	Pass (PPP#)	0.1231935
233	Possible	1.022601	Pass (PP?#)	0.1281673
234	Yes	0.3626659	Pass (PPP#)	0.1543471
235	Yes	0.555973	Pass (PPP#)	0.2657551
236	Yes	0.555973	Pass (PPP#)	0.2657551
237	Yes	0.555973	Pass (PPP#)	0.2657551
238	Possible	1.7473039	Pass (PP?#)	0.4759303
239	Yes	0.7996501	Pass (PPP#)	0.2643451
240	Possible	1.1505599	Pass (PP?#)	0.01640513
241	Possible	1.1876442	Pass (PP?#)	0.3833324
242	Possible	1.1104419	Pass (PP?#)	0.1842548
243	Possible	1.2339715	Pass (PP?#)	0.1075388
244	Yes	0.3428911	Pass (PPP#)	0.1512337
245	Yes	0.9878245	Pass (PPP#)	0.04488258
246	Possible	1.1876442	Pass (PP?#)	0.3833324
247	Yes	0.8892672	Pass (PPP#)	0.1231935
248	Possible	1.022601	Pass (PP?#)	0.1281673
249	Yes	0.68485	Pass (PPP#)	0.08948508
250	Possible	1.2261093	Pass (PP?#)	0.07781574
251	Possible	1.4559582	Pass (PP?#)	0.1709246
252	Possible	1.7274048	Pass (PP?#)	0.3727497
253	Yes	0.8892672	Pass (PPP#)	0.1231935
254	Possible	1.1505599	Pass (PP?#)	0.01640513
255	Possible	1.022601	Pass (PP?#)	0.1281673
256	Possible	1.4222331	Pass (PP?#)	0.293526
257	Yes	0.8419798	Pass (PPP#)	0.07460492
258	Yes	0.8419798	Pass (PPP#)	0.07460492

otherwise NO or FAIL. Thus any given spectrum is matched against all the available standard sets and spectra to be classified as a particular class should show a match (YES/PASS) against that particular standard set and no match (NO/FAIL) against all other sets. Thus, this methodology provides the most unambiguous discrimination. A typical match/mismatch table compared against benign standard sets is given in Table III. All spectra belonging to the benign condition show match (YES/PASS) and all other classes of spectra, normal

and malignant, show no match (NO/FAIL). Thus the results obtained in the study further support the efficacy of Raman spectroscopic methods in discrimination of normal, malignant, and benign breast tissues.

## CONCLUSION

Raman spectra obtained from normal and pathological tissues show significant differences. The spectral profile of normal tissues is indicative of higher levels

of lipids. In comparison, the spectral profile of pathological tissues, both benign and malignant, indicates the presence of more proteins and fewer lipids. Further, among the pathological tissues, malignant tissue contains relatively more lipids in comparison to benign tissue. These findings are in corroboration with our basic understanding that neoplastic processes are fundamentally more cellular and hence would biochemically be observed to have higher levels of protein. Also, benign tissue having more stromal components relative to the more cellular components of malignant tissue would explain our observation of relatively more lipid in malignant tissue in comparison to benign tissue. PCA is employed for developing discrimination methods. Scores of factor 1 provided a reasonable discrimination. The analysis is further finetuned by employing Mahalanobis distance and spectral residuals as discriminating parameters. Limit tests or computation of match-mismatch tables showed most unambiguous discrimination. Thus the results obtained in the study further supports the efficacy of Raman spectroscopic methods in discrimination of normal, malignant, and benign breast tissues. Perceptively, these results are significant as with improvement of technique (development of fiber-optic probes), reproducibility, and data analysis, development of objective, rapid, and minimally invasive Raman spectroscopic technique for breast cancer screening and diagnosis seems quite feasible.

This work is carried out under the project entitled: "Development of laser spectroscopy techniques for early detection and follow up of therapy in breast malignancy" No. 5/13/23/2003-NCD-III, Indian Council for Medical Research, Government of India. The authors (M.V.P.C. and K.K.K.) are thankful to ICMR for senior research fellowships. Ms. Keerthi and Mr. Chethan N. Anand are acknowledged for their technical assistance in the sample handling/preservation and data acquisition.

## REFERENCES

1. Max, P. D.; Freddie, B.; Ferlay, J.; Poala, P. *A Cancer J Clin* 2005, 55, 74–108.
2. Ciatto, S.; Rosselli, D. T. M.; Zappa, M. *Br J Cancer* 1995, 71, 337–339.
3. Esserman, L.; Cowley, H.; Eberie, C.; Eberle, C.; Kirkpatrick, A.; Chang, S.; Berbaum, K.; Gale, A. *J Natl Cancer Inst* 2002, 369–375.
4. Destounis, S. V.; DiNitto, P.; Logan-Young, W.; Bonaccio, E.; Zuley, M. L.; Willison, K. M. *Radiology* 2004, 232, 578–584.
5. Liberman, L.; Dershaw, D. D.; Rosen, P. P.; Abramson, A. F.; Deutch, B. M.; Hann, L. E. *Radiology* 1994, 192, 793–795.
6. Gupta, P. K.; Majumder, S. K.; Uppal, A. *Lasers Surg Med* 1997, 21, 417–422.
7. Majumder, S. K.; Gupta, P. K.; Jain, B.; Uppal, A. *Lasers Life Sci* 1998, 8, 249–264.
8. Yang, Y.; Katz, A.; Celmer, E. J.; Zurawska-Szczepaniak, M.; Alfano, R. R. *Photochem Photobiol* 1997, 66, 518–522.
9. Bigio, I. J.; Bown, S. G.; Briggs, G.; Kelley, C.; Lakhani, S.; Pickard, D.; Ripley, P. M.; Rose, I. G.; Saunders, C. J. *Biomed Opt* 2000, 5, 221–228.
10. Haka, A. S.; Volynskaya, Z.; Gardecki, J. A.; Nazemi, J.; Hicks, D.; Fitzmaurice, M.; Dasari, R. R.; Crowe, J. P.; Feld, M. S. *Cancer Res* 2006, 66, 3317–3322.
11. Abigail, S. H.; Shaefer-Peltier, K. E.; Maryann, F.; Joseph, C.; Dasari, R. R.; Feld, M. S. *Proc Natl Acad Sci U S A* 2005, 102, 12371–12376.
12. Abigail, S. H.; Shaefer-Peltier, K. E.; Maryann, F.; Crowe, J.; Dasari, R. R.; Feld, M. S. *Cancer Res* 2002, 62, 5375–5380.
13. Shaefer-Peltier, K. E.; Haka, A. S.; Fitzmaurice, M.; Crowe, J.; Myles, J.; Dasari, R. R.; Feld, M. S. *J Raman Spectrosc* 2002, 33, 552–563.
14. Shaefer-Peltier, K. E.; Haka, A. S.; Motz, J. T.; Fitzmaurice, M.; Dasari, R. R.; Feld, M. S. *J Cell Biochem* 2002, 87, S125–S137.
15. Kneipp, J.; Tom, B. S.; Kliffen, M.; Marian, M. P.; Puppels, G. *Vib Spectrosc* 2003, 32, 67–74.
16. Manoharan, R.; Shafer, K.; Perelman, I.; Wu, J.; Chen, K.; Deinum, G.; Fitzmaurice, M.; Myles, J.; Crowe, J.; Dasari, R. R.; Feld, M. S. *Photochem Photobiol* 1998, 67, 15–22.
17. Hanlon, E. B.; Manoharan, R.; Koo, T. W.; Shafer, K. E.; Motz, J. T.; Fitzmaurice, M.; Kramer, J. R.; Itzkan, I.; Dasari, R. R.; Feld, M. S. *Phys Med Biol* 2000, 45, R1–R59.
18. Murali Krishna, C.; Sockalingam, G. D.; Kurien, J.; Lakshmi, R.; Venteo, L.; Pluot, M.; Manfait, M.; Kartha, V. B. *Appl Spectrosc* 2004, 58, 107–114.
19. Murali Krishna, C.; Prathima, N. B.; Malini, R.; Vadhiraja, B. M.; Rani, Bhatt, A.; Donald, J. F.; Pralhad, K.; Vidyasagar, M. S.; Kartha, V. B. *Vib Spectrosc* 2006, 41, 136–141.
20. Malini, R.; Venkatakrishna, K.; Kurien, J.; Keethilatha Pai, M.; Kartha, V. B.; Murali Krishna, C. *Biopolymers* 2006, 81, 179–193.
21. Manjunath, B. K.; Kurien, J.; Rao, L.; Murali Krishna, C.; Chidananda, M. S.; Venkatakrishna, K.; Kartha, V. B. *J Photochem Photobiol B: Biology*, 2004, 73, 49–58.
22. Clark, R. J. H.; Hester, R. E. In *Advances in Spectroscopy*; New York: Wiley, 1993.
23. Parker, E. S. *Applications of Infrared and Raman and Resonance Raman Spectroscopy in Biochemistry*; New York: Plenum Press, 1983.
24. Mahalanobis, P. C. *Proc Natl Inst Sci India*, 1936, 2, 49.
25. Mark, H. L. *Anal Chem* 1987, 59, 790.
26. *PLSplus/IQ User's Guide*; Galactic Industries Corporation: Salem, New Hampshire, USA, 1999.

*Reviewing Editor: Laurence Nafie*